Supporting Information

Multifunctional Copper-Glutathione Clusters with Superior p-Nitrophenol Degradation and Horseradish Peroxidase-Like Activity

Mayowa Oyebanji[a], Xuejiao Yang[a], Ling Chen[a], Wencai Sun[a], Ruru Qian[a], Haizhu Yu[a*], Manzhou Zhu[a]

[a] *Department of Chemistry and Centre for Atomic Engineering of Advanced Materials, Key Laboratory of Structure and Functional Regulation of Hybrid Materials of Physical Science and Information Technology and Anhui Province Key Laboratory of Chemistry for Inorganic/Organic Hybrid Functionalized Materials, Anhui University, Hefei 230601, China.*

* Corresponding author: Prof. Haizhu Yu (E-mail: yuhaizhu@ahu.edu.cn)

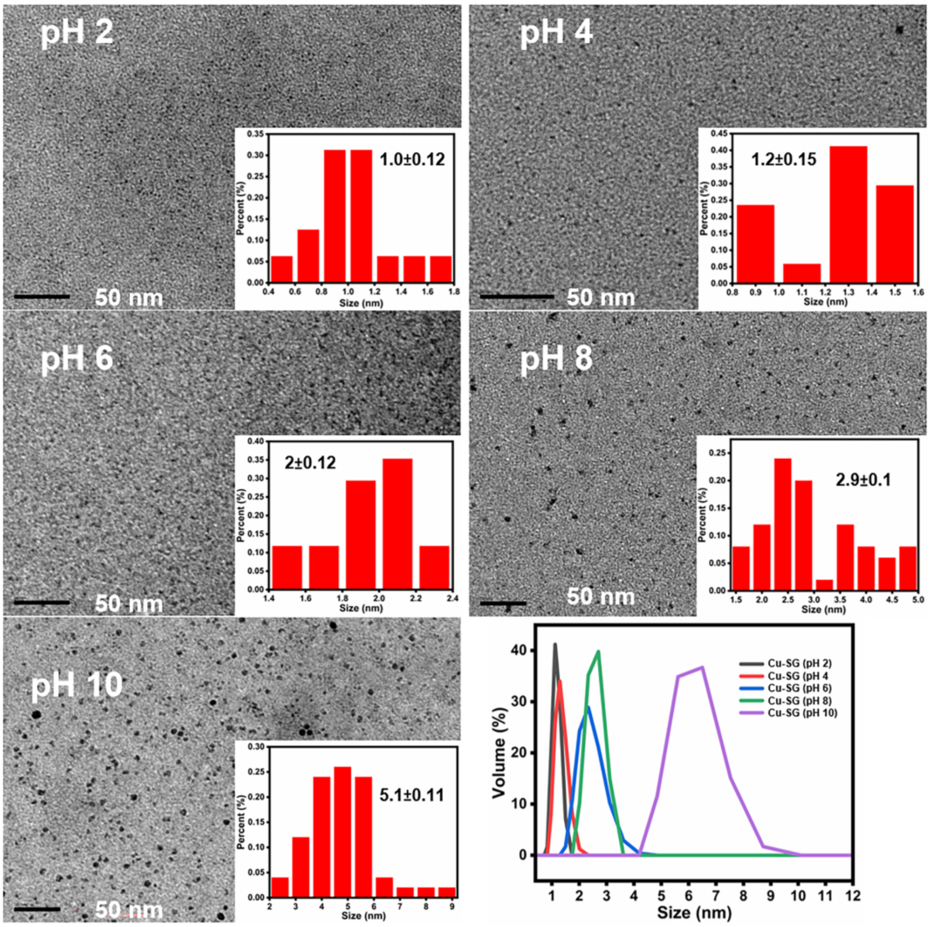

Fig. S1. TEM images of samples on acid etching (pH under different pH circumstance by acid-etching (insets: size distribution) and DLS analysis of the related samples.

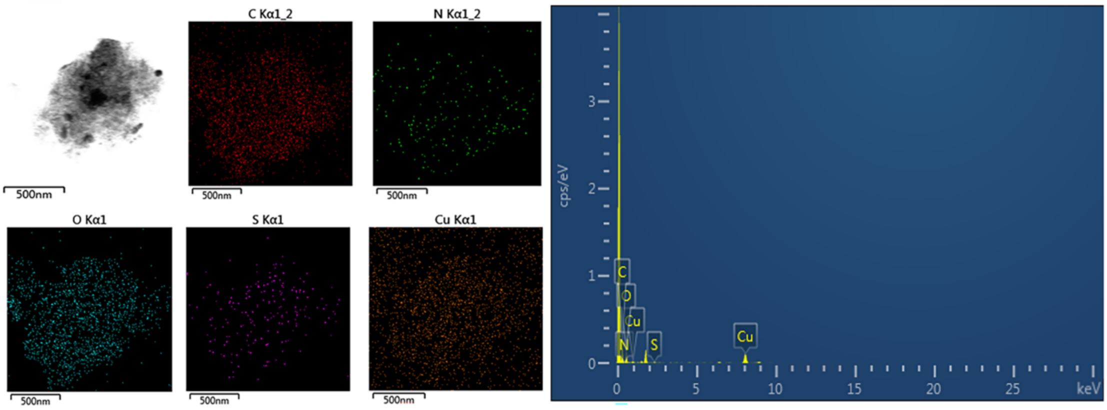

Fig. S2. EDS elemental mapping images and spectra of Cu-NPs.

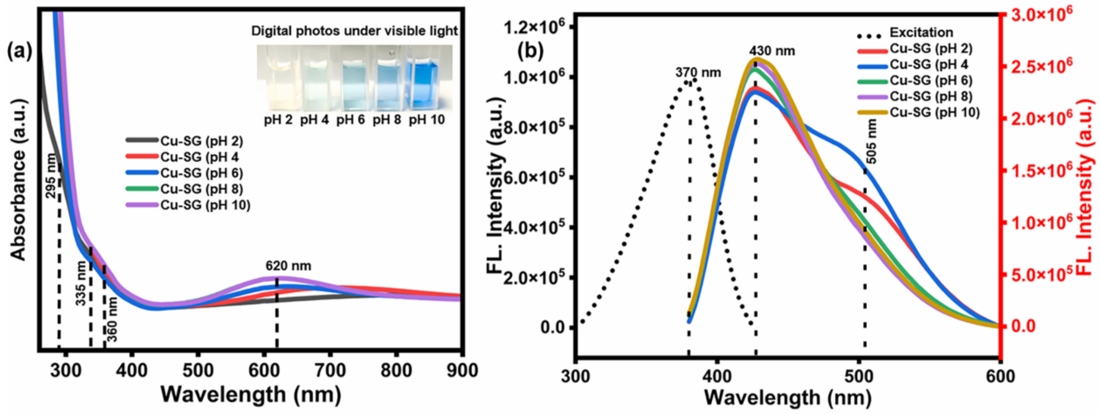

Fig. S3. a. UV-vis absorption spectra of Cu-SG on acid-etching (inset: corresponding digital photos under visible light). (b) Cu-SG fluorescence excitation at 370 nm (Black dash line) and emission curves (430 nm and 505 nm) on acid-etching.

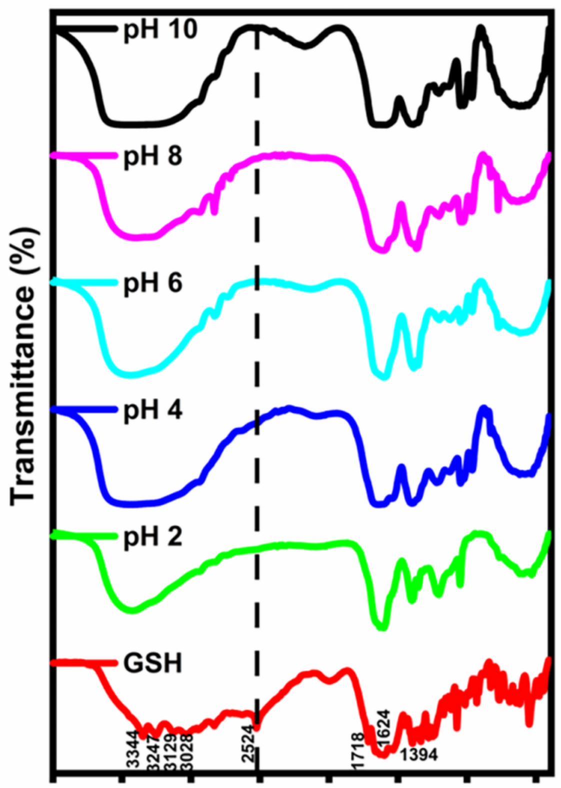

Fig. S4. FT-IR spectra of GSH and the cluster samples during acid-etching. According to the results, the -SH vibrational peak has been invisible in the Cu-NP state, and the acid etching makes little influence on the FT-IR peaks of GSH ligands.

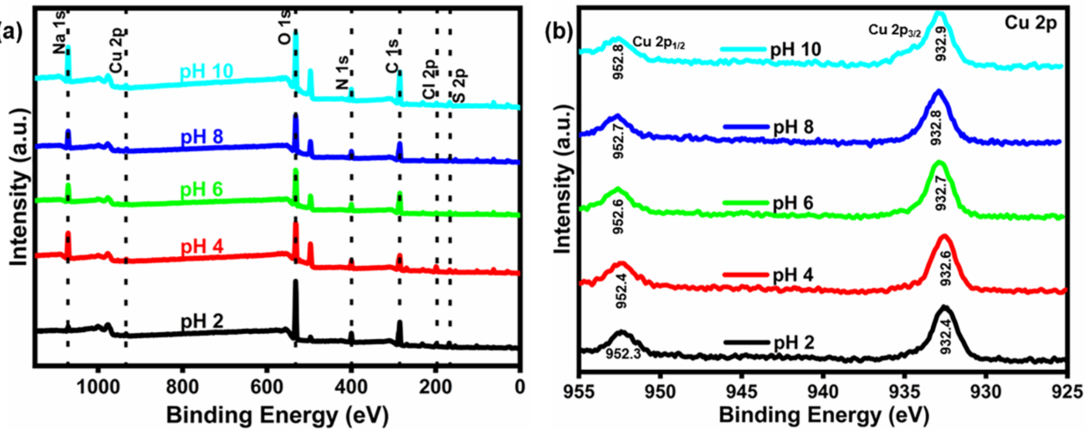

Fig. S5. (a) XPS full survey spectra of Cu-SG on acid-etching. (b) XPS spectra in the Cu 2p region of Cu-SG on acid-etching.

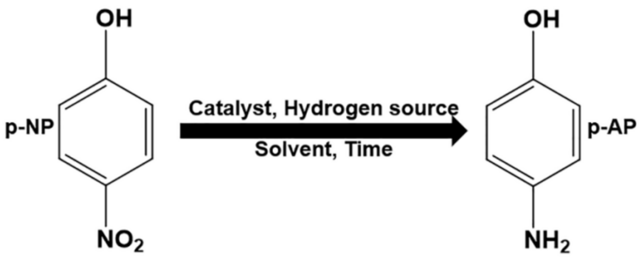

Scheme S1. The conversion scheme of p-NP to p-AP.

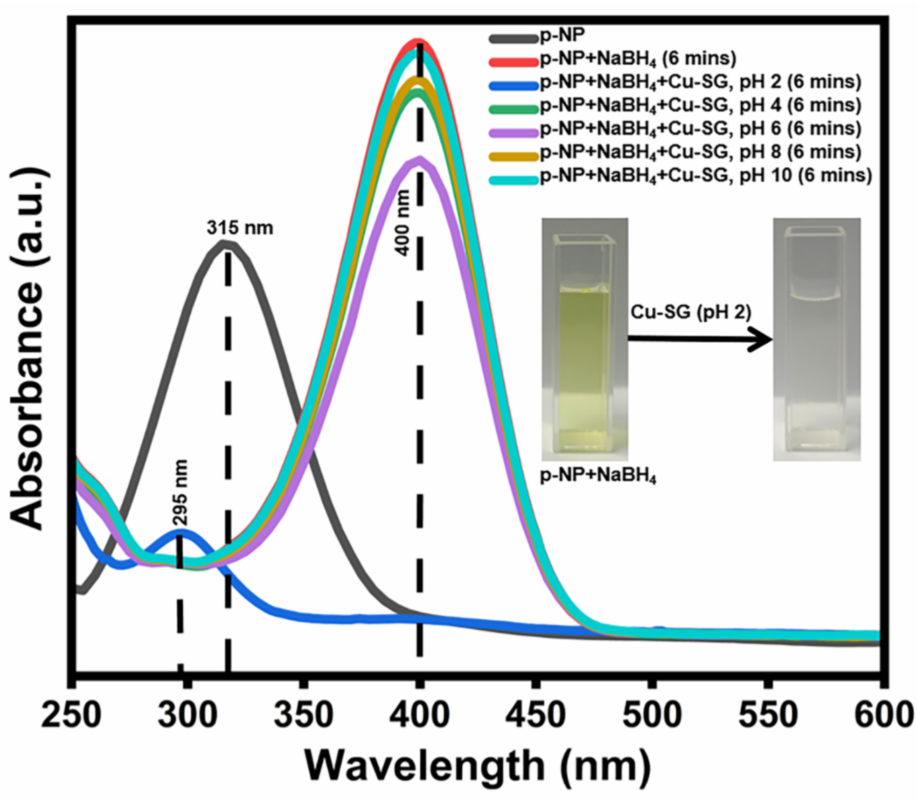

Fig. S6. p-NP reduction with Cu-SG on acid-etching.

Table S1. Cu-SG on acid-etching with catalytic performance for p-NP reduction.
Conversion = $(1 — A_t/A_0) \times 100$
A_0 and A_t represent the UV/vis absorbance (at 400 nm) of p-NP at time 0 and t, respectively.

Entry	Catalyst	Hydrogen source	Solvent	Time (min)	Conversion (%)
1	Cu-SG (pH 2)	$NaBH_4$	H_2O	6	>98
2	/	$NaBH_4$	H_2O	0	0
3	Cu-SG (pH 2)	/	H_2O	0	0
4	Cu-SG (pH 4)	$NaBH_4$	H_2O	6	<0.5
5	Cu-SG (pH 6)	$NaBH_4$	H_2O	6	<1
6	Cu-SG (pH 8)	$NaBH_4$	H_2O	6	<0.5
7	Cu-SG (pH 10)	$NaBH_4$	H_2O	6	<0.05

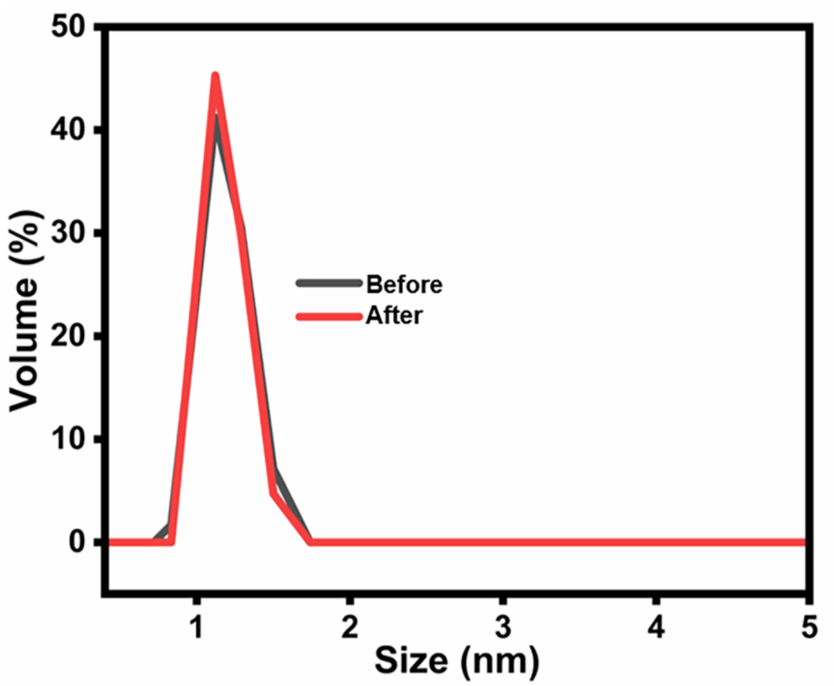

Fig. S7. DLS of Cu-SG before and after reaction with p-NP.

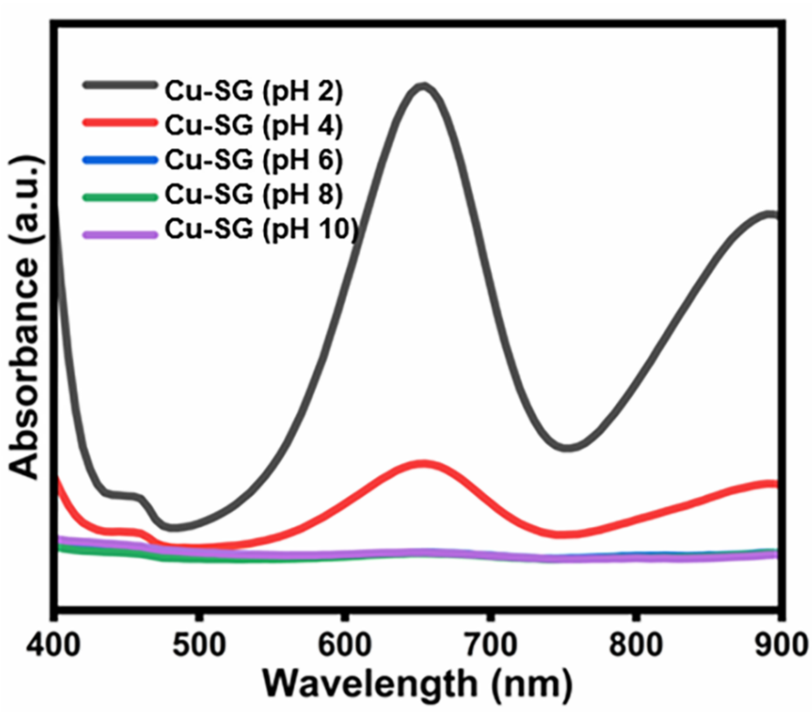

Fig. S8. HRP-like activity of Cu-SG on acid-etching (TMB+H_2O_2+Cu-SG (pH 2 - pH 10).

Table S2. A comparison of the kinetic parameters (K_m and V_{max}) determined for various HRP mimics nanomaterials.

Catalyst	H_2O_2		TMB		Ref.
	K_m [mM]	V_{max} [μM s^{-1}]	K_m [mM]	V_{max} [μM s^{-1}]	
SWNT	2.41	1.00	/	/	[1]
$Fe_{0.8}Ni_{0.2}S_2$	0.06	2.00	0.512	1.92	[2]
FeS_2	0.227	3.92	4.88	6.99	[3]
Cu SAzyme	9.89	3.85	0.38	0.48	[4]
Cu-CN	3.00	2.59	0.26	1.98	[5]
aCu(II)-CIFs	0.54	1.16	0.87	1.48	[6]
TO@Ru	7.680	1.35	/	/	[7]
HRP	3.70	0.87	0.43	1.00	[8]
Cu-SG	0.41	0.15	2.11	0.12	**This work**

Table S3. The Cu-SG probe performance compared to reported colorimetric based HRP-like nanomaterials for H_2O_2 detection.

HRP-like nanomaterials	**Linear range (μM)**	**LOD (μM)**	**Ref.**
M-CQDs	2-60	0.35	[9]
Ce/Zeolite	0-5	0.32	[10]
rGO/CM	1-10	0.15	[11]
Au NPs	0.02-0.7	12.33	[12]
Ce-MOF	4-16	10.00	[13]
TO@Ru	5-100	14.63	[7]
Cu-SG	0-40	6.03	**This work**

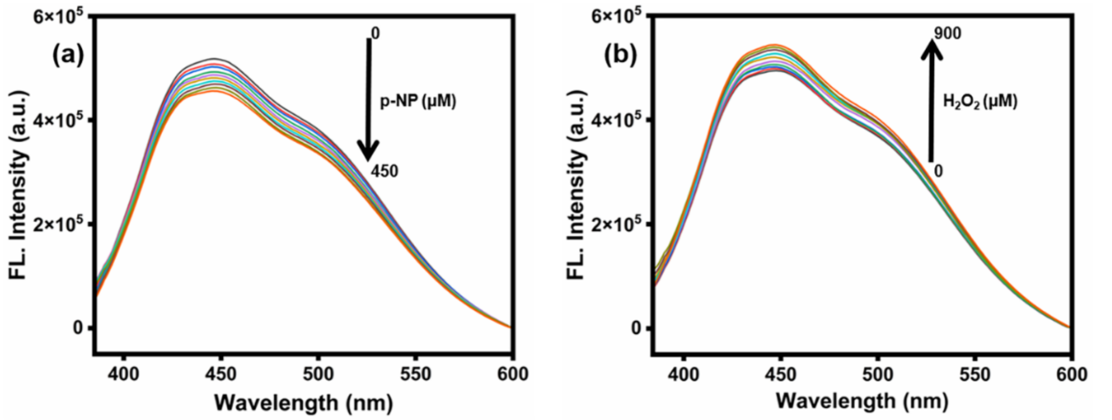

Fig. S9. (a) Fluorescence emission spectra of; (a) Cu-SG-p-NP and (b) Cu-SG- H_2O_2 systems at varying concentration of analytes (p-NP = 50, 100, 150, 200, 250, 300, 350, 400, and 450 μM; H_2O_2 = 100, 200, 300, 400, 500, 600, 700, 800, and 900 μM) at λ_{ex} = 370 nm, T = 298 K.

References

(1) Wang, X.; Gao, X. J.; Qin, L.; Wang, C.; Song, L.; Zhou, Y.-N.; Zhu, G.; Cao, W.; Lin, S.; Zhou, L.; et al. eg occupancy as an effective descriptor for the catalytic activity of perovskite oxide-based peroxidase mimics. *Nat. Commun.* **2019**, *10* (1), 704. DOI: 10.1038/s41467-019-08657-5.

(2) Zhang, C.; Nan, Z. 2D/3D-Shaped Fe0.8Ni0.2S2/ZIF-67 as a Nanozyme for Rapid Measurement of H2O2 and Ascorbic Acid with a Low Limit of Detection. *Inorg. Chem.* **2022**, *61* (35), 13933-13943. DOI: 10.1021/acs.inorgchem.2c01925.

(3) Huang, X.; Xia, F.; Nan, Z. Fabrication of FeS2/SiO2 Double Mesoporous Hollow Spheres as an Artificial Peroxidase and Rapid Determination of H2O2 and Glutathione. *ACS Appl. Mater. Interfaces* **2020**, *12* (41), 46539-46548. DOI: 10.1021/acsami.0c12593.

(4) Chang, M.; Hou, Z.; Wang, M.; Wen, D.; Li, C.; Liu, Y.; Zhao, Y.; Lin, J. Cu Single Atom Nanozyme Based High-Efficiency Mild Photothermal Therapy through Cellular Metabolic Regulation. *Angew. Chem. Int. Ed.* **2022**, *61* (50), e202209245. DOI: 10.1002/anie.202209245.

(5) Liu, J.; Wang, X.; Ma, F.; Yang, X.; Liu, Y.; Zhang, X.; Guo, S.; Wang, Z.; Yang, S.; Zhao, R. Atomic copper(I)-carbon nitride as a peroxidase-mimic catalyst for high selective detection of perfluorooctane sulfonate. *Chem. Eng. J.* **2022**, *435*, 134966. DOI: 10.1016/j.cej.2022.134966.

(6) Ding, Z.; Gao, X.; Yang, Y.; Wei, H.; Yang, S.; Liu, J. Amorphous copper(II)-cyanoimidazole frameworks as peroxidase mimics for hydrogen sulfide assay. *J. Colloid Interface Sci.* **2023**, *652*, 1889-1896. DOI: 10.1016/j.jcis.2023.09.014.

(7) Zhu, H.; Deng, J.; Mu, S.; Xiao, S.; Li, Q.; Wang, W.; Gao, Y.; Luo, X.; Gao, S.; Cheng, C. Creating peroxidase-mimetic clusterzymes for efficient and selectively enzymatic diagnosis of biomarkers. *Chem. Eng. J.* **2023**, *462*, 142215. DOI: 10.1016/j.cej.2023.142215.

(8) Gao, L.; Zhuang, J.; Nie, L.; Zhang, J.; Zhang, Y.; Gu, N.; Wang, T.; Feng, J.; Yang, D.; Perrett, S.; et al. Intrinsic peroxidase-like activity of ferromagnetic nanoparticles. *Nature Nanotechnology* **2007**, *2* (9), 577-583. DOI: 10.1038/nnano.2007.260.

(9) Chandra, S.; Singh, V. K.; Yadav, P. K.; Bano, D.; Kumar, V.; Pandey, V. K.; Talat, M.; Hasan, S. H. Mustard seeds derived fluorescent carbon quantum dots and their peroxidase-like activity for colorimetric detection of H2O2 and ascorbic acid in a real sample. *Anal. Chim. Acta* **2019**, *1054*, 145-156. DOI: 10.1016/j.aca.2018.12.024.

(10) Cheng, X.; Huang, L.; Yang, X.; Elzatahry, A. A.; Alghamdi, A.; Deng, Y. Rational design of a stable peroxidase mimic for colorimetric detection of H2O2 and glucose: A synergistic CeO2/Zeolite Y nanocomposite. *J. Colloid Interface Sci.* **2019**, *535*, 425-435. DOI: 10.1016/j.jcis.2018.09.101.

(11) Singh, G.; Kushwaha, A.; Sharma, M. Intriguing peroxidase-mimic for H2O2 and glucose sensing: A synergistic Ce2(MoO4)3/rGO nanocomposites. *J. Alloys Compd.* **2020**, *825*, 154134. DOI: 10.1016/j.jallcom.2020.154134.

(12) Ding, Y.; Yang, B.; Liu, H.; Liu, Z.; Zhang, X.; Zheng, X.; Liu, Q. FePt-Au ternary metallic nanoparticles with the enhanced peroxidase-like activity for ultrafast colorimetric detection of H2O2. *Sens. Actuators B Chem.* **2018**, *259*, 775-783. DOI: 10.1016/j.snb.2017.12.115.

(13) Wei, X.; Li, Y.; Qi, S.; Chen, Y.; Yin, M.; Zhang, L.; Tian, X.; Gong, S.; Wang, F.; Zhu, Y.; et al. Ce-MOF Nanosphere as Colorimetric Sensor with High Oxidase Mimicking Activity for Sensitive Detection of H2O2. *J. Inorg. Organomet. Polym. Mater.* **2022**, *32* (9), 3595-3600. DOI: 10.1007/s10904-022-02422-w.